

e-Blood

mpeg1 promoter transgenes direct macrophage-lineage expression in zebrafishFelix Ellett,^{1,2} Luke Pase,¹ John W. Hayman,¹ Alex Andrianopoulos,³ and Graham J. Lieschke¹¹Cancer and Haematology Division, Walter and Eliza Hall Institute of Medical Research, Melbourne, Australia; ²Department of Medical Biology, University of Melbourne, Australia; and ³Department of Genetics, University of Melbourne, Melbourne, Australia

Macrophages and neutrophils play important roles during the innate immune response, phagocytosing invading microbes and delivering antimicrobial compounds to the site of injury. Functional analyses of the cellular innate immune response in zebrafish infection/inflammation models have been aided by transgenic lines with fluorophore-marked neutrophils. However, it has not been possible to study macrophage behaviors

and neutrophil/macrophage interactions in vivo directly because there has been no macrophage-only reporter line. To remove this roadblock, a macrophage-specific marker was identified (*mpeg1*) and its promoter used in *mpeg1*-driven transgenes. *mpeg1*-driven transgenes are expressed in macrophage-lineage cells that do not express neutrophil-marking transgenes. Using these lines, the different dynamic behaviors of neutrophils and

macrophages after wounding were compared side-by-side in compound transgenics. Macrophage/neutrophil interactions, such as phagocytosis of senescent neutrophils, were readily observed in real time. These zebrafish transgenes provide a new resource that will contribute to the fields of inflammation, infection, and leukocyte biology. (*Blood*. 2011;117(4):e49-e56)

Introduction

After injury or infection, the first line of defense against invading pathogens is the innate immune system. During the inflammatory response, interaction between the cells of the innate immune system is critical for correct coordination of phases of cellular influx and resolution.¹

The zebrafish has proven to be a very useful tool for modeling innate immune responses.² Leukocyte behavior can be directly observed in optically transparent zebrafish embryos and larvae, and transgenic zebrafish strains have enabled particular cellular behaviors to be visualized in vivo with an ease and precision unparalleled in other vertebrate models. Detailed examination of inflammation and host-pathogen interactions at the cellular level has been enabled by several transgenic strains marking embryonic and adult neutrophils, such as Tg(*mpx*:EGFP)^{3,4} and *lyz*-driven transgenes.^{5,6} Such lines have been used to study neutrophil responses and fluxes during infection^{7,8} and during acute and chronic inflammation.^{3,4,9} Combinations of these approaches have provided some important new insights (eg, regarding the role of leukocytes in mycobacterial infection).¹⁰⁻¹³

In contrast to the availability of neutrophil-reporter zebrafish lines for more than 5 years, no line has yet been developed that specifically labeled macrophages, one of the most important cell types of the innate immune system. Direct in vivo imaging of embryonic and larval macrophages has been possible by identifying cells on the basis of size, location, motility, and behavior.^{10,14-17} The Tg(*ftla*:EGFP) line¹⁸ expresses in primitive leukocytes as well as endothelial cells, and this has been exploited to examine primitive macrophage behavior in wounded embryos.¹⁹ In Tg(*mpx*:EGFP) zebrafish, a subpopulation of cells with duller fluorescence than its more brightly fluorescent neutrophils, has been character-

ized as macrophages.²⁰ The absence of a specific reporter line for macrophages per se has been an ongoing hindrance to comprehensive analyses of the cellular innate immune response in this model organism.

Macrophage expressed gene 1 (*mpeg1*) was first identified as a gene with expression tightly restricted to human and murine macrophages,²¹ and has subsequently been used as a marker for this cell lineage in mammalian systems²² and zebrafish.²³ These studies present transgenic constructs and lines based on the zebrafish *mpeg1* promoter that drive transgene expression specifically in zebrafish embryonic macrophages, allowing visualization of macrophage behavior in vivo. Specificity of transgene expression is demonstrated in transient and stable transgenic embryos. Transgene utility is demonstrated by imaging and quantifying several macrophage behavioral dynamics and by a comparative analysis of macrophage and neutrophil behaviors and interactions after wounding. The exchange of large cytoplasmic portions from living neutrophils to living macrophages in vivo is described for the first time.

Methods

Zebrafish

Adults and embryos were maintained and studied at 28°C. The AB strain was used for transgenesis. Other zebrafish lines used were Tg(*mpx*:EGFP)^{i14,3} Tg(*lyz*:EGFP)^{nz117,5} Tg(*lyz*:dsRed)^{nz50,5}, and Tg(UAS-E1b:Kaede)^{s1999t,24} Animal protocols were approved by the Walter and Eliza Hall Institute Animal Ethics Committee. All embryos were treated with 0.003% 1-phenyl-2-thiourea (Sigma-Aldrich) from 8 hpf.

Submitted October 18, 2010; accepted October 25, 2010. Prepublished online as *Blood* First Edition paper, November 17, 2010; DOI 10.1182/blood-2010-10-314120.

The online version of this article contains a data supplement.

The publication costs of this article were defrayed in part by page charge payment. Therefore, and solely to indicate this fact, this article is hereby marked "advertisement" in accordance with 18 USC section 1734.

© 2011 by The American Society of Hematology

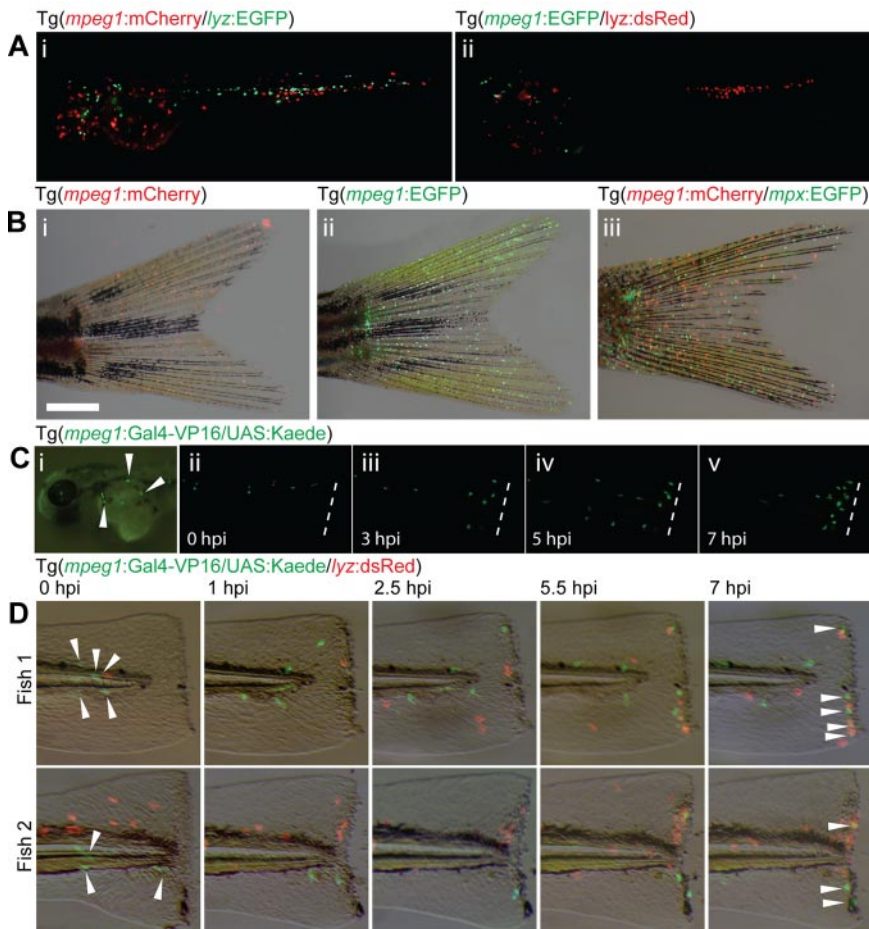


Figure 1. A 1.86-kb *mpeg1* promoter fragment drives transient transgene expression in macrophages.

(A) Transient mosaic transgene expression in embryos injected with tol2-flanked *Tg(mpeg1:mCherry)* (i) and *Tg(mpeg1:EGFP)* (ii) DNA constructs into *Tg(lyz:EGFP)* and *Tg(lyz:dsRed)* transgenic backgrounds, respectively. The experiment was conducted on *Tg(lyz:EGFP)* and *Tg(lyz:dsRed)* embryos to provide comparison and nonoverlap of expression with neutrophils. (B) Transgene expression in F0 adults injected with tol2-flanked *Tg(mpeg1:mCherry)* (i,iii) and *Tg(mpeg1:EGFP)* (ii) DNA constructs. (iii) *Tg(mpeg1:mCherry)* was introduced onto the *Tg(impx:EGFP)* background to provide comparison and nonoverlap of expression with neutrophils. (C) Transient transgene expression resulting from delivery of a tol2-flanked *Tg(mpeg1:Gal4-VP16)* construct into *Tg(UAS:Kaede)* embryos results in expression of Kaede in dispersed cells (i) that migrate in response to wounding (tail transection) (ii-v). Time: hours post injury (hpi). (D) Delivery of tol2-flanked *Tg(mpeg1:Gal4-VP16)* into *Tg(UAS:Kaede/lyz:dsRed)* embryos allows comparison of macrophage (green, arrowheads) and neutrophil populations (red) migrating in response to wounding (tail transection). Time: hours post injury (hpi).

Gene expression analysis

Expression data were surveyed in an online database²⁵ and confirmed by whole-mount in situ hybridization as previously described^{26,27} using an antisense riboprobe corresponding to nucleotides -3 to 453 of *mpeg1* cDNA sequence. Other riboprobes were *csf1r*²⁸ and *mpx*.²⁹

mpeg1 promoter identification and cloning

Zebrafish genome assembly Zv8 (http://www.ensembl.org/Danio_rerio/) informed primer design for amplification of 30437143–30438999 nt from chromosome 8, generating 1.86 kb of sequence corresponding to the immediately proximal *mpeg1* 5'-untranslated region. Cloning used Gateway methods and vectors.³⁰ Supplemental Table 1 (available on the *Blood* Web site; see the Supplemental Materials link at the top of the online article) lists promoter and riboprobe primer sequences.

Microinjection and transgenesis

mpeg1 transgenesis was performed using Gateway protocols for Tol2-mediated recombination.³⁰ Antisense morpholino oligonucleotides were obtained from GeneTools (www.gene-tools.com) and microinjected at 200 to 500 μ M into 1- or 2-cell embryos at 1.7 nL per bolus (morpholino oligonucleotide sequences in supplemental Table 1).

Leukocyte function studies

For wounding, tails were transected coronally by scalpel blade at 3 dpf²⁹ and embryos mounted in 1.5% low melting agarose. Imaging commenced approximately 4 minutes after injury. For neutral red staining, embryos were incubated in egg water with 2.5 μ g/mL neutral red for 12 hours.³¹ To demonstrate phagocytosis, *Penicillium marneffei* spores were prepared as

described.³² Spores were heat-killed at 70°C for 15 minutes. Calcofluor staining was performed by incubation of spores in 10mM Calcofluor White (Sigma-Aldrich) for 15 minutes, followed by several rounds of washing and resuspension in normal saline. A total of 10 to 20 spores/embryo were microinjected into the somatic muscle of 3 dpf embryos and imaging commenced 20 minutes later.

Microscopy and image analysis

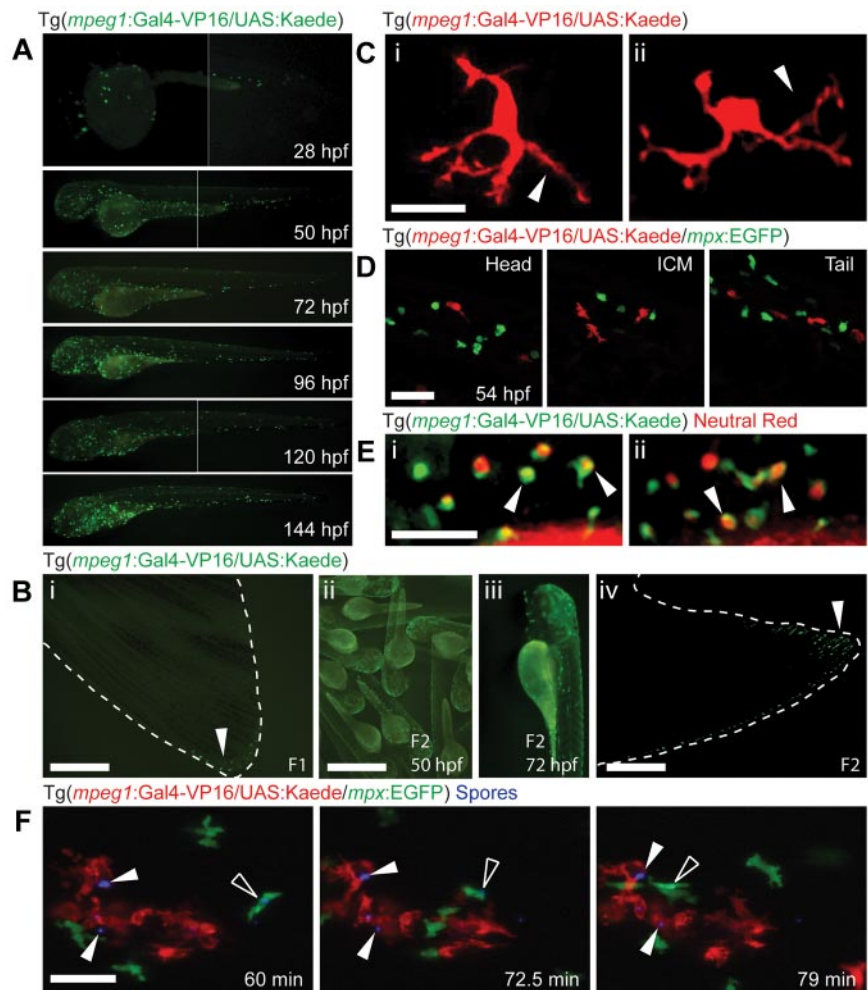
For dissecting microscopy (Figures 1, 2A-B,E), an Olympus SZX16 microscope with a DP71 camera and 1 \times (Figures 1, 2A-B) and 2 \times (Figure 2E) objectives was used. Filter sets used: enhanced green fluorescent protein/unconverted Kaede: SZX2-FGFPHQ (excitation, 460-480 nm; emission, 495-540 nm); dsRed/photoconverted Kaede/Neutral Red: SZX2-RFP2 (excitation, 540-580 nm; emission, 610 nm); and Kaede photoconversion: CFP CHR-U-N49001 (Chroma; excitation, 434-438 nm, emission 440-520 nm, exposure, 15-20 minutes). Original images were 1360 \times 1024 RGB color (cropped).

For single photon confocal microscopy (Figure 2C-D), an Olympus FV1000-BX61WI upright multiphoton with an XLUMPlan F1 20 \times , water immersion, 0.95 NA objective was used. Excitation wavelengths used were 473 nm for EGFP and 559 nm for Kaede. Original image details were, for Figure 2Ci, xyz: 512 \times 512 \times 37 pixels, maximum intensity projection (cropped); for Figure 2Cii, xyz: 512 \times 512 \times 34 pixels, maximum intensity projection (cropped); for Figure 2D, (head) xyz: 512 \times 512 \times 113 pixels, maximum intensity projection; for Figure 2D, (ICM) xyz: 512 \times 512 \times 105 pixels, maximum intensity projection; and for Figure 2D (Tail) xyz: 512 \times 512 \times 140 pixels, maximum intensity projection.

Line-scanning confocal microscopy (Figures 2F, 3A, and Figure 4), was performed using a Zeiss LSM 5 Live inverted microscope with a Plan-Apochromat 20 \times , 0.8 NA objective. Wavelengths used were: 405 nm

Figure 2. Macrophage ontology, morphology, and behavior in stable *mpeg1* transgenic zebrafish.

(A) Unconverted Kaede expression (green) in dispersed macrophages in *Tg(mpeg1:Gal4-VP16/UAS:Kaede)* F1 embryos from 28 to 144 hpf. Images at 28, 50, and 120 hpf are composites assembled from photographs of the same embryo taken in 2 focal planes. (B) Loss of transgene expression occurs in young F1 and F2 *Tg(mpeg1:Gal4-VP16/UAS:Kaede)* adults (i,iv), demonstrated by the absence of dispersed fluorescent macrophages in the tail fin; compare with macrophages in the tail fins of *Tg(mpeg1:mCherry)* and *Tg(mpeg1:EGFP)* F0 animals in Figure 1B. However, the direct offspring of an outcross of the F1 adult (i) still shows strong embryonic transgene expression in dispersed macrophages (ii,iii). (i,iv) Arrowheads indicate autofluorescent iridophores. Bar represents 1 mm. (C) Dendritic morphology (arrowheads) of photoconverted Kaede (red) marked cells in *Tg(mpeg1:Gal4-VP16/UAS:Kaede)* F1 embryos. Bar represents 20 μ m. (D) No overlap of fluorophore expression was observed between photoconverted Kaede and EGFP in F1 *Tg(mpeg1:Gal4-VP16/UAS:Kaede/mpx:EGFP)* compound transgenic embryos, demonstrating that the *mpeg1* promoter drives expression in an entirely separate myeloid cell population to that of the *mpx* promoter (green represents neutrophils; and red, macrophages). Bar represents 50 μ m. (E) Macrophage pinocytosis leads to accumulation of neutral red staining in vacuoles of unconverted *Tg(mpeg1:Gal4-VP16/UAS:Kaede)* positive cells (green) in the brain (arrowheads) of F1 embryos. Bar represents 50 μ m. (F) Phagocytosis of heat-killed *Penicillium marneffei* spores (calcofluor-labeled, blue, arrowhead) by macrophages (red represents photoconverted Kaede) and neutrophils (green represents EGFP). Note phagocytosis of lower fungal spore by macrophage (bottom filled arrowhead) and migration of neutrophil with intracellular spore (open arrowhead). Stills from supplemental Video 1. Bar represents 50 μ m. Time: minutes after infection.



for Calcofluor; 488 nm for EGFP; and 561 nm for photoconverted Kaede. Original image details were, for Figure 2F, xyt: $512 \times 512 \times 4$ (pixels) \times 100 (2 frames per minute) maximum intensity projection (cropped, deconvoluted); for Figure 3A, xyt: $512 \times 512 \times 1$ (pixels) \times 1138 (2 frames per minute); for Figure 4A, xyt: $512 \times 512 \times 1$ (pixels) \times 1138 (2 frames per minute; cropped); and for Figure 4B-D, xyt: $512 \times 512 \times 1$ (pixels) \times 1800 (2 frames per minute) (cropped).

Wide-field microscopy for cell-tracking studies (Figure 3) was performed using a Nikon Ti-E inverted microscope with a Plan Fluor 10 \times , 0.3 NA objective. Wavelength filters used were FITC (Nikon; excitation 465-495 nm; emission, 515-565) for EGFP and TRITC (Nikon; excitation 515-565 nm; emission 550-660) for photoconverted Kaede. Original image details were Figure 3B-H, xyt: $512 \times 512 \times 4$ (pixels, $2 \times$ binning) \times 1080, 1 frame per minute). Deconvolution and maximum intensity projection were performed before tracking analysis.

Images were processed in Adobe Creative Suite CS4 and ImageJ, Version 1.4q, programs for presentation. Quantitative leukocyte behavior measurements were extracted using Metamorph (Series 7.5). The “meandering index” is as previously defined (linear distance between start and finish points divided by actual path length).³³ The “in-wound persistence index” was defined as the percentage of remaining time in a time lapse that a cell spent at the wound edge after arrival.

Statistics

Descriptive and analytical statistics were prepared in Prism 5, Version 5.0a (GraphPad Software). Data are mean \pm SD unless otherwise stated.

Results

Myeloid expression of *mpeg1*

In a search of an online database²⁵ for genes with potentially leukocyte-restricted expression in zebrafish whose promoters might be useful for making new transgenic lines, *mpeg1* attracted interest in for its expression at 20 hours post fertilization (hpf) to 5 days post fertilization (dpf) in cells dispersed in a typical pattern for leukocytes.²⁹

Our initial whole-mount in situ hybridization characterization of *mpeg1* expression until 78 hpf confirmed this pattern (supplemental Figure 1A). MO knockdown studies demonstrated that, as expected of a gene expressed in myeloid cells, *mpeg1* expression was dependent on *spil/pu.1*³⁴ and *csf3r*³⁵ signaling (supplemental Figure 1B). On this basis, fragments of its promoter were cloned. A recent independent study has also characterized zebrafish *mpeg1* as a gene with highly restricted, specific expression in macrophages up to 48 hpf.²³

These data collectively indicate that *mpeg1* is expressed in dispersed early zebrafish leukocytes with macrophage-lineage restriction. The macrophage lineage specificity of *mpeg1* expression has been further demonstrated by its promoter activity as characterized in “The *mpeg1* promoter drives transgene expression in macrophages.”

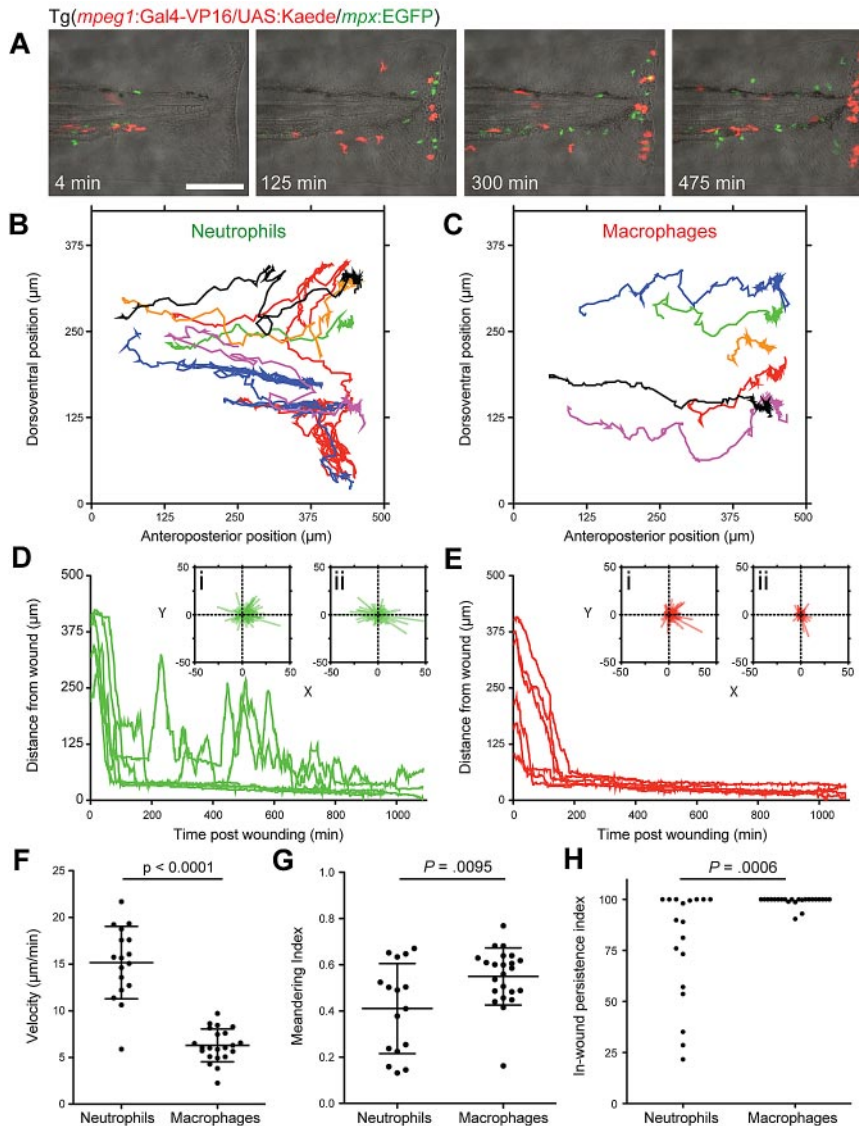


Figure 3. Comparative descriptive and quantitative analysis of macrophage and neutrophil behavior after wounding. (A) Frames extracted from 11.5 hours of time lapse microscopy (supplemental Video 2) after tail transection in a Tg(*mpeg1:Gal4-VP16/UAS:Kaede/mpx:EGFP*) F1 embryo (red represents macrophages; and green, neutrophils). Bar represents 100 μm . (B-C) Cell migration paths for the first 6 neutrophils (B) and 6 macrophages (C) to arrive at the wound, followed for 18 hours after tail transection, extracted from a video of another wounded Tg(*mpeg1:Gal4-VP16/UAS:Kaede/mpx:EGFP*) F1 transgenic embryo. (D-H) Graphing of distance to wound edge for the same 6 neutrophils (D) and macrophages (E) as in panels B and C demonstrates an overall difference in migratory and dwelling behaviors. All macrophages migrate directly to the wound and remain near the wound edge for the remainder of the time course, whereas approximately 30% of neutrophils resume a roaming behavior from 3 to 6 hours after wounding. Insets i and ii for each panel present collected x/y movement vectors before (i) and after (ii) wound arrival. Strong directionality is demonstrated by both cell types before arrival, but macrophages move with a slower prearrival velocity (F) and with a stronger directionality reflected by their higher meandering index (direct path length/actual path length) (G). In-wound persistence index, the percentage of remaining time spent at the wound edge after arrival (H), demonstrates the propensity of macrophages to remain in the wound margin for long periods after their arrival, whereas neutrophils show a significantly larger spread of behaviors. Descriptive statistics: (B-E) Data for the same 6 cells of each type. (F-H) Data points are individual cells from 4 embryos imaged for 18 hours after wounding. (F,G) Bars represent mean plus or minus SD. Tests of significance: (F,G) *t* test, 2-tailed. (H) Mann-Whitney test, 2-tailed.

The *mpeg1* promoter drives transgene expression in macrophages

Several *mpeg1*-driven, tol2-flanked transgene constructs were built for recapitulating *mpeg1* expression in live animals: Tg(*mpeg1:EGFP*); Tg(*mpeg1:mCherry*); and Tg(*mpeg1:Gal4-VP16*). In F0-microinjected embryos, transgene expression was observed in a dispersed population of mobile, putative myeloid cells (Figure 1A-C). Inflammation assays using F0 Tg(*mpeg1:Gal4-VP16/UAS:Kaede*) embryos demonstrated Kaede-expressing cells migrating in response to wounding (Figure 1C-D), a characteristic leukocyte behavior. Encouragingly, in F0s, no overlap of fluorophore expression was observed between *mpeg1*-driven transgenes and characterized neutrophil-specific Tg(*mpx:EGFP*) and *lyz*-driven transgenes (Figure 1A-B,D), although these F0 embryos were potentially mosaic.

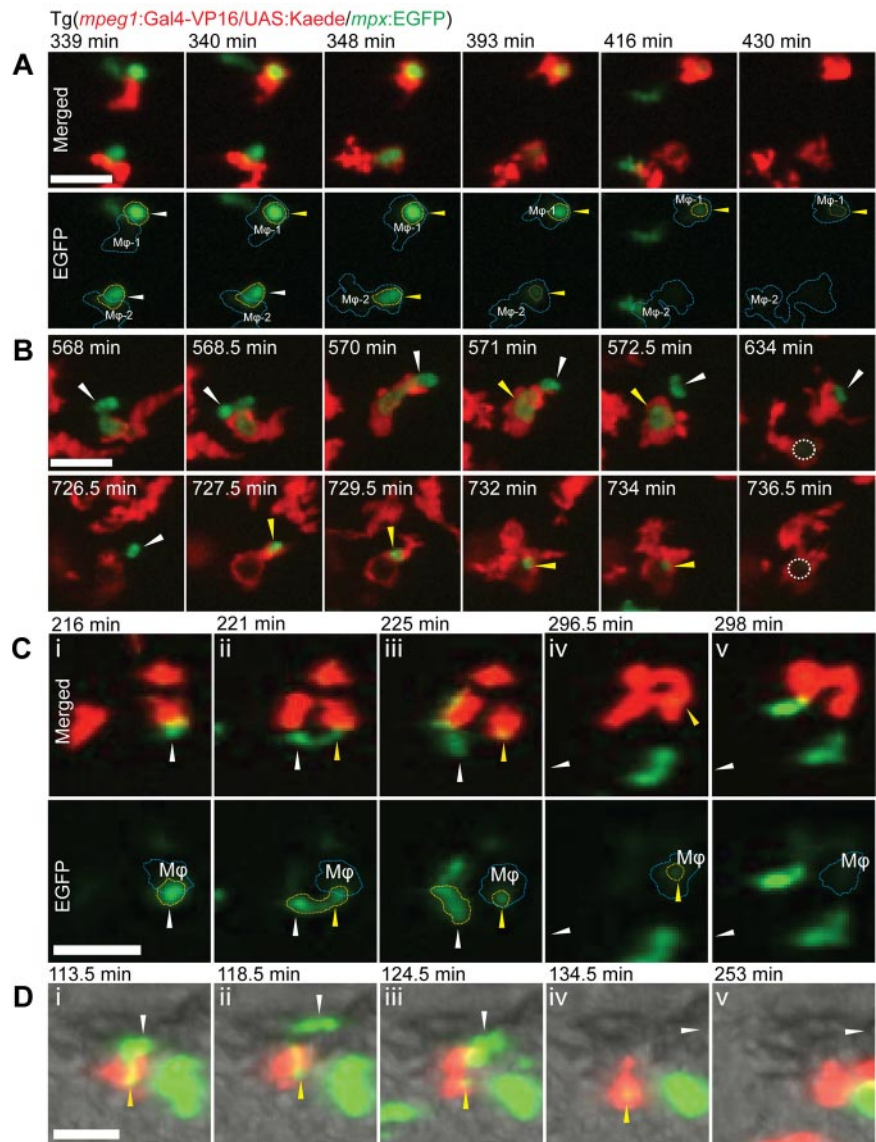
Stable germline transgenic Tg(*mpeg1:Gal4-VP16*) zebrafish were generated to provide opportunity for this promoter to drive a range of effector gene functionalities (Figure 2). Initial transgenesis was performed on a Tg(*UAS:Kaede*) background. *mpeg1*-transgene-marked cells were present into early larval stages of F0, F1 (Figure 2A), and F2 embryos (Figure 2Bii-iii). However, transgene expressing cells were observed only rarely in Tg(*mpeg1:Gal4-VP16/UAS:*

Kaede) F1 and F2 adults (Figure 2Bi,iv). In contrast, Tg(*mpeg1:mCherry*) and Tg(*mpeg1:EGFP*) F0 adults showed strong transgene expression (Figure 1B).

To assess overlap between expression of the new *mpeg1*-driven transgene and a standard neutrophil marker in nonmosaic F1s, F0 founders were crossed into the Tg(*mpx:EGFP*) line³ and compound transgenic Tg(*mpeg1:Gal4-VP16/UAS:Kaede/mpx:EGFP*) F1 embryos were imaged after photoconversion of Kaede. No overlap at all was observed between cell populations in the embryos at 2, 3, or 7 dpf (number of scored cells expressing *mpeg1/mpx*both: at 2 dpf, 50/125/0; at 3 dpf, 60/306/0; at 7 dpf, 222/401/0; scores collected from multiple fields in ≥ 2 embryos), establishing that in this line the *mpeg1* promoter drives expression exclusively in a nonneutrophil cell population (Figure 2D).

The fluorescent cells in Tg(*mpeg1:Gal4-VP16/UAS:Kaede*) embryos had several defining morphologic and functional attributes characteristic of macrophage-lineage cells. They were large cells with extensive cytoplasmic extensions (50-100 μm including branches, Figure 2C). Incubation with neutral red led to accumulation of stain via pinocytosis (Figure 2E), as previously described for primitive zebrafish macrophages.³¹ The cells were phagocytic: injection of calcofluor-stained fungal conidia into the

Figure 4. Interactions between macrophages and neutrophils in vivo. (A) Interactions between macrophages (red represents photoconverted Kaede) and neutrophils (green represents EGFP) in *Tg(mpeg1:Gal4-VP16/UAS:Kaede/mpx:EGFP)* compound transgenic F1 embryos. Two examples of apoptotic neutrophils being phagocytosed by macrophages at the wound margin. The first occurs at 340 minutes by macrophage 1 (M ϕ -1) at the top of frame followed by the second at 348 minutes by M ϕ -2. Loss of green neutrophil fluorescence is evident in the M ϕ -1 after 76 minutes and within M ϕ -2 occurs in 45 minutes. Stills from supplemental Video 3. Bar represents 10 μ m. (B) Demonstration that the loss of cytoplasmic neutrophil fluorescence is dependent on macrophage phagocytosis. At 568 to 571 minutes, partial phagocytosis of a segment of a neutrophil. At 572.5 to 634 minutes, loss of fluorescence in the phagocytosed fragment occurs after approximately 6 hours (dotted circle represents region of lost EGFP fluorescence). Providing an internal control for this process, an unphagocytosed still-fluorescing neutrophil fragment remains stationary throughout the first phagocytic phase, until it is subsequently engulfed by the same macrophage at 727.5 minutes, with loss of its EGFP fluorescence at 736.5 minutes. Stills from supplemental Video 4. Bar represents 10 μ m. In both panels, white arrowheads and yellow arrowheads indicate unphagocytosed and phagocytosed states, respectively, of neutrophil corpse. (C-D) Two examples of cytoplasmic transfer from live neutrophils (green represents EGFP) to macrophages (red represents photoconverted Kaede). (C) A neutrophil/macrophage interaction near a wound margin results in a cytoplasmic fragment from a live neutrophil transferring to within a macrophage. (Top panel) Merged images. (Bottom panel) EGFP channel only. Dashed outlines indicate position of macrophage (blue) and neutrophil/fragment. Stills extracted from supplemental Video 5. Bar represents 20 μ m. (D) A neutrophil/macrophage interaction in the trunk of the embryo. Merged fluorescence and bright-field images clearly demonstrate interaction resulting in cytoplasm transfer from neutrophil to macrophage. Stills from supplemental Video 6. Bar represents 20 μ m. In both examples, white arrowheads and yellow arrowheads indicate unphagocytosed and phagocytosed states, respectively, of the transferring neutrophil cytoplasmic fragment. Neutrophil viability throughout the process is demonstrated by its subsequent migration out of the field of view (direction of white arrow in subpanels iv and v).



trunk led to migration of marked cells to the wound site and phagocytosis of microbes (Figure 2F; supplemental Video 1).

During inflammation, macrophages migrate with different kinetics to neutrophils

F1 *Tg(mpeg1:Gal4-VP16/UAS:Kaede/mpx:EGFP)* transgenic embryos were wounded and imaged, using photoconverted Kaede (red) to discriminate macrophages from EGFP-expressing (green) neutrophils (Figure 3, supplemental Video 2).

During the arrival phase, both neutrophils and macrophages migrated toward the site of injury with strong directionality, demonstrated by their tracks (Figure 3B-C) and arrival movement vectors (Figure 3Di,Ei) during migration. Compared with the swift initial neutrophil migration toward the wound averaging 15 μ m/minute, macrophages were significantly tardier, extending more pseudopodia and migrating more slowly (6 μ m/minute; Figure 3F; supplemental Video 2). Macrophages took a more direct route to the wound margin, reflected in a significantly higher meandering index (0.55) than neutrophils (0.4; Figure 3G). Macrophages arriving at the wound in the first 24 hours remained for as long as 4 days after wounding, a behavior proven by localized photo-

conversion of Kaede at the wound site and monitoring cell location thereafter (supplemental Figure 2B-C), substantially extending previous observations.^{36,37} Additional macrophages continued to arrive until at least 48 hours after wounding (supplemental Figure 2C). In contrast, neutrophils discontinued directional migration toward the wound after 6 hours (Figure 3A; supplemental Video 2).

Neutrophils and macrophages also behaved differently after arrival at the wound. During 18-hour time lapses, approximately 30% of neutrophils that arrived at the wound margin resumed a roaming behavior from 3 to 6 hours after wounding (Figure 3D,H), whereas more than 90% macrophages dwelt persistently at the wound margin after their arrival (Figure 3E,H).

These data demonstrate the utility of this new transgenic zebrafish line, in combination with other transgenes, to observe, compare, and quantify distinctive macrophage behaviors.

Live cell imaging of macrophage-neutrophil interactions during inflammation

With both neutrophils and macrophages marked by distinguishable fluorophores, neutrophil/macrophage interactions in vivo can be

observed dynamically. One such behavior is the phagocytosis of apoptotic neutrophils during inflammation resolution, previously investigated statically in fixed zebrafish.³⁷ After tail transection, this interactive behavior was readily observed in living Tg(*mpeg1*:Gal4-VP16/UAS:Kaede/*mpx*:EGFP) embryos, after photoconversion of Kaede to red fluorescence (Figure 4A; supplemental Video 3). On neutrophil arrival at the wound margin, some take on the rounded morphology previously attributed to an apoptotic cell.³⁷ With the subsequent arrival of macrophages, some engaged in direct, complex, intertwining, behavior with such neutrophils, resulting in their apparent phagocytosis with loss of neutrophil EGFP fluorescence. Sometimes only part of the neutrophil cytoplasm detached and disappeared (Figure 4B; supplemental Video 4). Viewed in real-time, the ongoing cellular protrusion and movement of neutrophils indicate that these neutrophils are not always completely dead before their phagocytosis by macrophages (supplemental Video 3).

Fluorophore loss in neutrophils has been attributed to cell death, possibly after phagocytosis,³⁷ although separation of these events has not previously been possible. Observations in vivo in these compound transgenic lines strongly support the notion that fluorophore loss most often represents phagocytosis by macrophages. After neutrophil spherification, loss of fluorescence occurred after a median of 70.5 minutes (range, 6.5–472 minutes; n = 9) in phagocytosed cells, whereas unphagocytosed cells were rarely observed to lose fluorescence independently. In a particularly instructive example, only a portion of a neutrophil was initially phagocytosed, with subsequent loss of fluorescence in only that portion; the remaining portion retained its fluorescence until it too was later phagocytosed (Figure 4B; supplemental Video 4). This example indicates that neutrophil fluorescence can be maintained even in immobile cell fragments and that macrophage phagocytosis results in loss of EGFP protein activity.

Macrophages interacted directly with actively motile, living neutrophils. An unexpected occasional outcome of these interactions was the transfer of portions of fluorescent cytoplasm from neutrophil to macrophage (Figure 4C-D; supplemental Videos 5-6). The direction of transfer was always from a donor neutrophil to a recipient macrophage. The viability of the donor neutrophil in such exchanges was demonstrated by its ongoing active pseudopodial activity and its subsequent migration away from the site of the interaction (Figure 4C-D; supplemental Videos 5-6). The detached neutrophil cytoplasmic fragment was not just coincidentally superimposed on a macrophage because, after detachment from a neutrophil, its subsequent movement was in concert with that of the macrophage (supplemental Video 7; supplemental Video 6 examined in slow motion). After its transfer to macrophages, the cytoplasmic fragment lost fluorescence (Figure 4Cv,Dv).

Discussion

Previously, to mark zebrafish macrophages, several genes and/or their promoters have been used. However, the degree of overlap of expression of various leukocyte-expressed genes in different leukocyte subtypes has been an ongoing point of confusion in the field for some time. Some markers originally considered to be macrophage-specific later appeared less specific as the number of markers for leukocyte subtypes expanded and coexpression was examined. Expression of the *csflr* gene²⁸ has become a commonly used benchmark for defining macrophage identity, but a transgenic line using its promoter is not yet described. However, as this gene is

expressed in neural crest cells as well, full recapitulation of its promoter activity for transgenic expression of a fluorophore would also be expected to mark this nonmacrophage cell type. Macrophages have also been identified by elimination: on the basis of nonoverlapping expression between pan-leukocytic markers, such as *l-plastin* (*lcp1*) and neutrophil-specific expression of *mpx*.^{20,38} Cells expressing low levels of EGFP in the Tg(*mpx*:EGFP)^{uwm1} line display macrophage characteristics²⁰; in our hands, a similar population is discernable by confocal microscopy in the Tg(*mpx*:EGFP)ⁱ¹¹⁴ line (data not shown). Markers based on early fate-specification genes, such as *spi1*, do not have leukocyte sublineage specificity and are limited in expression timeframe.³⁹ Descriptions of *lyz*-driven transgene expression in macrophages^{5,6} required reevaluation given the complete overlap of *lyz* expression with *mpx*,⁴⁰ and in the context of our new data. Recently, *mpeg1* and *cxc3.2* were reported as genes with tight macrophage-specific expression in zebrafish,²³ based on static expression studies.

For the first time in zebrafish embryos, with these new *mpeg1*-driven transgenes, macrophage-specific transgene expression has been achieved. *mpeg1*-driven transgene expression is nonoverlapping with the neutrophil-specific transgenes driven from *mpx* and *lyz* promoters. This allows for clear separation of embryonic zebrafish leukocyte populations by different fluorophores. These tools provide for a wide range of experimental utility in embryonic zebrafish. The macrophage-constraining *mpeg1* promoter functionality resides in a 1.86-kb DNA fragment, making its recloning and reuse highly practical. Because the fluorophore reporter constructs are in a tol-2 vector, high-level mosaic transient expression can be achieved, meaning that a subset of macrophages at least can be marked in extant compound transgenic backgrounds by microinjection alone, without complex interbreeding. Judging from its performance in transient assays, the promoter fragment is strong and not generally susceptible to off-target expression. The first *mpeg1*-driven stable transgenic line provides the versatility of the Gal4-VP16 transactivator; hence, any currently available or desired UAS-effector transgene functionality can now be engaged for macrophage-specific expression.

Several issues may affect the stability of the germline Tg(*mpeg1*:Gal4-VP16/UAS:Kaede) reporter line we have made, although they do not undermine its current utility or the usefulness of the constructs themselves for transient macrophage labeling. There is a possibility of genetic drift resulting from segregation in subsequent generations if there are multiple integration sites in the Tg(*mpeg1*:Gal4-VP16) founder. To date, we have not recognized any overt toxicity in macrophages resulting from mechanisms, such as squelching (ie, transcription factor sequestration).⁴¹ Although there is strong embryonic and larval transgene expression, to date we have not been able to demonstrate reporter transgene activity in adult kidney and spleen macrophages by direct fluorescence microscopy in the compound Tg(*mpeg1*:Gal4-VP16/UAS-Kaede) fish (Figure 2B; data not shown). Comparison with directly driven transgene constructs demonstrates that this loss of expression is unique to the Gal4-VP16/UAS based system and most probably reflects somatic transgene silencing. Embryos produced by these F0 and F1 adults exhibit full transgene expression, suggesting that silencing occurs somatically and does not affect expression in embryos/larvae of subsequent generations. Epigenetic transgene silencing has been observed in other zebrafish Gal4-UAS systems, although more related to CpG-rich concatamerized UAS sequences⁴² than to the Gal4 driver line. Despite this, this reporter line appears sustainably useful for studies in embryos and larvae.

Videos of side-by-side neutrophil and macrophage behaviors after wounding display, in real time and in vivo, the strikingly different dynamics of each cell type. Although some aspects of these different behaviors have previously been inferred from static studies and other models, the simplicity and elegance of these transgenic fish provide advantages. These include the internally controlled observations made in single animals and opportunity for quantification. Previous zebrafish studies of neutrophil flux after wounding sought to demonstrate the fate of apoptotic neutrophils using fixed embryos and costaining of TdT-mediated dUTP nick end labeling and neutrophil material within cells positive for the pan-leukocytic marker *lcp1*.³⁷ The interaction between macrophages and senescing or dead, but still-fluorescent, Tg(*mpx*:EGFP) neutrophil corpses can now be examined directly in real time in vivo.

The extent of the direct, dynamic interaction between living macrophages and neutrophils revealed in these embryos was surprising, particularly the occasional exchange of substantial fragments of fluorophore-marked neutrophil cytoplasm from living neutrophils to macrophages. Several features of this exchange distinguish it from several other previously described neutrophil processes. As well as identifying the phenomenon, these studies provide tools that will enable examination of hypotheses about its function. The extent to which one cell-type's behavior may be dependent on another can now also be explored, in embryos and larvae at least, by deleting the macrophage lineage: by the combination of Tg(*mpeg1*:Gal4-VPI6) fish and UAS:deleter-gene constructs, such as Tg(UAS:nitroreductase).⁴³

The lack of a macrophage-specific transgenic zebrafish has constrained zebrafish-based research, particularly in the field of innate immunity. The *mpeg1*-driven transgenic lines allow for: specific inducible ablation of macrophages; macrophage-specific overexpression of transgenes; fluorescence-activated cell sorter and analysis of macrophages as a pure population; imaging of interactions between macrophages and other immune cells in vivo; interaction studies between macrophages and intracellular pathogens, such as *Mycobacterium marinum* and *Candida albicans*; reexamination of macrophage roles in inflammation, wound healing, and development; their interactions with other cell types (eg, vasculature, muscle) in vivo; and macrophage-focused chemical genetic screens. Transgenes using this new zebrafish promoter

represent a major step forward for the study of macrophage behavior and function in vivo.

Acknowledgments

The authors thank Ethan Scott, Herwig Baier, Stephen Renshaw, Chris Hall, and Phil Crosier for transgenic lines; Cameron Nowell and Kelly Rogers for assistance with imaging; Harshini Weerasinghe and Sony Varma for technical assistance; Mark Greer, Kelly Turner, and Prue Chamberlain for animal care in the aquarium; Ben Kile, Joan Heath, and Ben Croker for discussions; Steve Jane, David Curtis, and the Royal Melbourne Hospital Bone Marrow Research Laboratory for support. Microscopy used instruments in the Center for Advanced Microscopy (Ludwig Institute for Cancer Research) and the Australian Cancer Research Foundation Center for Therapeutic Target Discovery.

This work was supported by the National Institutes of Health (grant R01 HL079545) and the National Health and Medical Research Council (grant 637394; G.J.L.). F.E. was supported by an Australian Postgraduate Award and Walter and Eliza Hall Institute of Medical Research Edith Moffatt Scholarship. Walter and Eliza Hall Institute of Medical Research receives infrastructure support from the Commonwealth National Health and Medical Research Council Independent Research Institutes Infrastructure Support Scheme (361646) and a Victorian State Government Operational Infrastructure Support Scheme grant.

Authorship

Contribution: G.J.L. and F.E. conceived the project and wrote the manuscript; F.E. assessed candidate genes, built the constructs, performed microinjections, and characterized the lines; L.P. provided advice on experimental design and performed live cell imaging; J.W.H. performed some in situ hybridization experiments; A.A. provided fungal spores; and all authors discussed the project, interpreted data, and commented on the manuscript.

Conflict-of-interest disclosure: The authors declare no competing financial interests.

Correspondence: Graham J. Lieschke, Australian Regenerative Medicine Institute, Monash University, Victoria 3800, Australia; e-mail: Lieschke@monash.edu.

References

- Soehnlein O, Lindbom L. Phagocyte partnership during the onset and resolution of inflammation. *Nat Rev Immunol*. 2010;10(6):427-439.
- van der Sar AM, Appelmelk BJ, Vandenbroucke-Grauls CM, Bitter W. A star with stripes: zebrafish as an infection model. *Trends Microbiol*. 2004;12(10):451-457.
- Renshaw SA, Loynes CA, Trushell DM, Elworthy S, Ingham PW, Whyte MK. A transgenic zebrafish model of neutrophilic inflammation. *Blood*. 2006;108(13):3976-3978.
- Mathias JR, Perrin BJ, Liu TX, Kanki J, Look AT, Huttenlocher A. Resolution of inflammation by retrograde chemotaxis of neutrophils in transgenic zebrafish. *J Leukoc Biol*. 2006;80(6):1281-1288.
- Hall C, Flores MV, Storm T, Crosier K, Crosier P. The zebrafish lysozyme C promoter drives myeloid-specific expression in transgenic fish. *BMC Dev Biol*. 2007;7:42.
- Zhang Y, Bai XT, Zhu KY, et al. In vivo interstitial migration of primitive macrophages mediated by JNK-matrix metalloproteinase 13 signaling in response to acute injury. *J Immunol*. 2008;181(3):2155-2164.
- Phennicie RT, Sullivan MJ, Singer JT, Yoder JA, Kim CH. Specific resistance to *Pseudomonas aeruginosa* infection in zebrafish is mediated by the cystic fibrosis transmembrane conductance regulator. *Infect Immun*. 2010;78(11):4542-4550.
- Vergunst AC, Meijer AH, Renshaw SA, O'Callaghan D. Burkholderia cenocepacia creates an intramacrophage replication niche in zebrafish embryos, followed by bacterial dissemination and establishment of systemic infection. *Infect Immun*. 2010;78(4):1495-1508.
- Mathias JR, Dodd ME, Walters KB, et al. Live imaging of chronic inflammation caused by mutation of zebrafish Hai1. *J Cell Sci*. 2007;120(19):3372-3383.
- Clay H, Davis JM, Beery D, Huttenlocher A, Lyons SE, Ramakrishnan L. Dichotomous role of the macrophage in early *Mycobacterium marinum* infection of the zebrafish. *Cell Host Microbe*. 2007;2(1):29-39.
- Volkman HE, Pozos TC, Zheng J, Davis JM, Rawls JF, Ramakrishnan L. Tuberculous granuloma induction via interaction of a bacterial secreted protein with host epithelium. *Science*. 2010;327(5964):466-469.
- Davis JM, Ramakrishnan L. The role of the granuloma in expansion and dissemination of early tuberculous infection. *Cell*. 2009;136(1):37-49.
- Ellett F, Lieschke GJ. Zebrafish as a model for vertebrate hematopoiesis. *Curr Opin Pharmacol*. 2010;10(5):563-570.
- Levrud JP, Disson O, Kissa K, et al. Real-time observation of listeria monocytogenes-phagocytosis interactions in living zebrafish larvae. *Infect Immun*. 2009;77(9):3651-3660.
- Herbomel P, Thisse B, Thisse C. Ontogeny and behaviour of early macrophages in the zebrafish embryo. *Development*. 1999;126(17):3735-3745.
- Davis JM, Clay H, Lewis JL, Ghori N, Herbomel P,

- Ramakrishnan L. Real-time visualization of mycobacterium-macrophage interactions leading to initiation of granuloma formation in zebrafish embryos. *Immunity*. 2002;17(6):693-702.
17. van der Sar AM, Stockhammer OW, van der Laan C, Spaik HP, Bitter W, Meijer AH. MyD88 innate immune function in a zebrafish embryo infection model. *Infect Immun*. 2006;74(4):2436-2441.
 18. Lawson ND, Weinstein BM. In vivo imaging of embryonic vascular development using transgenic zebrafish. *Dev Biol*. 2002;248(2):307-318.
 19. Redd MJ, Kelly G, Dunn G, Way M, Martin P. Imaging macrophage chemotaxis in vivo: studies of microtubule function in zebrafish wound inflammation. *Cell Motil Cytoskeleton*. 2006;63(7):415-422.
 20. Mathias JR, Dodd ME, Walters KB, Yoo SK, Ranheim EA, Huttenlocher A. Characterization of zebrafish larval inflammatory macrophages. *Dev Comp Immunol*. 2009;33(11):1212-1217.
 21. Spilsbury K, O'Mara MA, Wu WM, Rowe PB, Symonds G, Takayama Y. Isolation of a novel macrophage-specific gene by differential cDNA analysis. *Blood*. 1995;85(6):1620-1629.
 22. Karlsson KR, Cowley S, Martinez FO, Shaw M, Minger SL, James W. Homogeneous monocytes and macrophages from human embryonic stem cells following coculture-free differentiation in M-CSF and IL-3. *Exp Hematol*. 2008;36(9):1167-1175.
 23. Zakrzewska A, Cui C, Stockhammer OW, Benard EL, Spaik HP, Meijer AH. Macrophage-specific gene functions in Spi1-directed innate immunity. *Blood*. 2010;116(3):e1-e11.
 24. Scott EK, Mason L, Arrenberg AB, et al. Targeting neural circuitry in zebrafish using GAL4 enhancer trapping. *Nat Methods*. 2007;4(4):323-326.
 25. Thisse B, Thisse C. Fast release clones: a high throughput expression analysis. ZFIN Direct Data Submission. <http://zfinfo.org>. 2004. Accessed April 2009.
 26. Lieschke GJ, Oates AC, Paw BH, et al. Zebrafish SPI-1 (PU.1) marks a site of myeloid development independent of primitive erythropoiesis: implications for axial patterning. *Dev Biol*. 2002;246(2):274-295.
 27. Oates AC, Brownlie A, Pratt SJ, et al. Gene duplication of zebrafish JAK2 homologs is accompanied by divergent embryonic expression patterns: only jak2a is expressed during erythropoiesis. *Blood*. 1999;94(8):2622-2636.
 28. Parichy DM, Ransom DG, Paw B, Zon LI, Johnson SL. An orthologue of the kit-related gene *fms* is required for development of neural crest-derived xanthophores and a subpopulation of adult melanocytes in the zebrafish, *Danio rerio*. *Development*. 2000;127(14):3031-3044.
 29. Lieschke GJ, Oates AC, Crowhurst MO, Ward AC, Layton JE. Morphologic and functional characterization of granulocytes and macrophages in embryonic and adult zebrafish. *Blood*. 2001;98(10):3087-3096.
 30. Kwan KM, Fujimoto E, Grabher C, et al. The Tol2kit: a multisite gateway-based construction kit for Tol2 transposon transgenesis constructs. *Dev Dyn*. 2007;236(11):3088-3099.
 31. Herbomel P, Thisse B, Thisse C. Zebrafish early macrophages colonize cephalic mesenchyme and developing brain, retina, and epidermis through a M-CSF receptor-dependent invasive process. *Dev Biol*. 2001;238(2):274-288.
 32. Canovas D, Andrianopoulos A. Developmental regulation of the glyoxylate cycle in the human pathogen *Penicillium marneffei*. *Mol Microbiol*. 2006;62(6):1725-1738.
 33. Lin A, Loughman JA, Zinselmeyer BH, Miller MJ, Caparon MG. Streptolysin S inhibits neutrophil recruitment during the early stages of *Streptococcus pyogenes* infection. *Infect Immun*. 2009;77(11):5190-5201.
 34. Rhodes J, Hagen A, Hsu K, et al. Interplay of PU.1 and *gata1* determines myelo-erythroid progenitor cell fate in zebrafish. *Dev Cell*. 2005;8(1):97-108.
 35. Liongue C, Hall CJ, O'Connell BA, Crosier P, Ward AC. Zebrafish granulocyte colony-stimulating factor receptor signaling promotes myelopoiesis and myeloid cell migration. *Blood*. 2009;113(11):2535-2546.
 36. Cvejic A, Hall C, Bak-Maier M, et al. Analysis of WASp function during the wound inflammatory response: live-imaging studies in zebrafish larvae. *J Cell Sci*. 2008;121(19):3196-3206.
 37. Loynes CA, Martin JS, Robertson A, et al. Pivotal advance: pharmacological manipulation of inflammation resolution during spontaneously resolving tissue neutrophilia in the zebrafish. *J Leukoc Biol*. 2010;87(2):203-212.
 38. Walters KB, Green JM, Surfus JC, Yoo SK, Huttenlocher A. Live imaging of neutrophil motility in a zebrafish model of WHIM syndrome. *Blood*. 2010;116(15):2803-2811.
 39. Ward AC, McPhee DO, Condron MM, et al. The zebrafish *spi1* promoter drives myeloid-specific expression in stable transgenic fish. *Blood*. 2003;102(9):3238-3240.
 40. Meijer AH, van der Sar AM, Cunha C, et al. Identification and real-time imaging of a myc-expressing neutrophil population involved in inflammation and mycobacterial granuloma formation in zebrafish. *Dev Comp Immunol*. 2008;32(1):36-49.
 41. Koster RW, Fraser SE. Tracing transgene expression in living zebrafish embryos. *Dev Biol*. 2001;233(2):329-346.
 42. Goll MG, Anderson R, Stainier DY, Spradling AC, Halpern ME. Transcriptional silencing and reactivation in transgenic zebrafish. *Genetics*. 2009;182(3):747-755.
 43. Pisharath H. Validation of nitroreductase, a pro-drug-activating enzyme, mediated cell death in embryonic zebrafish (*Danio rerio*). *Comp Med*. 2007;57(3):241-246.